Mean Structure and Fluctuations of the Kuroshio East of Taiwan

from In Situ and Remote Observations

By Yiing Jang Yang, Sen Jan, Ming-Huei Chang, Joe Wang,
Vigan Mensah, Tien-Hsia Kuo, Cheng-Ju Tsai,
Chung-Yaung Lee, Magdalena Andres, Luca R. Centurioni,
Yu-Heng Tseng, Wen-Der Liang, and Jian-Wu Lai
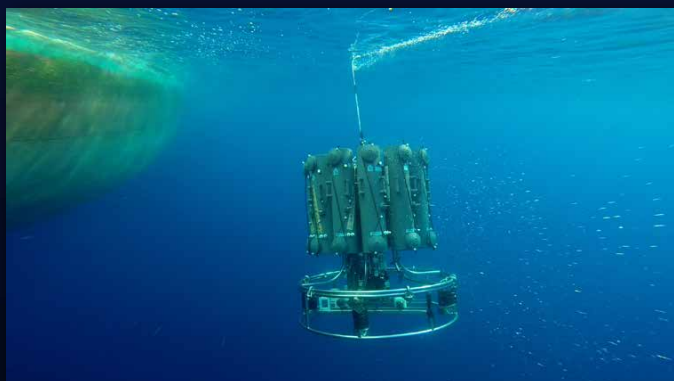
(background photo) R/V *Ocean Researcher I* (*OR1*) sailing in the Kuroshio east of Taiwan. (top left inset) The swift current of the Kuroshio causes a white "bubble line" on the sea surface after passing the wire connecting the CTD. (bottom left inset) Recovered mooring with fish school surrounding the buoy. (right inset) A 45" float with ADCP inside just popped up from 550 m depth to the sea surface. *Photo credits: Sen Jan, Chen-Jia Lien, and Yiing Jang Yang*

ABSTRACT. The Kuroshio is important to climate, weather prediction, and fishery management along the northeast coast of Asia because it transports tremendous heat, salt, and energy from east of the Philippines to waters southeast of Japan. In the middle of its journey northward, the Kuroshio's velocity mean and its variability east of Taiwan crucially affect its downstream variability. To improve understanding of the Kuroshio there, multiple platforms were used to collect intensive observations off Taiwan during the three-year Observations of the Kuroshio Transports and their Variability (OKTV) program (2012–2015). Mean Kuroshio velocity transects show two velocity maxima southeast of Taiwan, with the primary velocity core on the onshore side of the Kuroshio exhibiting a mean maximum velocity of ~1.2 m s^{-1}. The two cores then merge and move at a single velocity maximum of ~1 m s^{-1} east of Taiwan. Standard deviations of both the directly measured poleward (*v*) and zonal (*u*) velocities are ~0.4 m s^{-1} in the Kuroshio main stream. Water mass exchange in the Kuroshio east of Taiwan was found to be complicated, as it includes water of Kuroshio origin, South China Sea Water, and West Philippine Sea Water, and it vitally affects heat, salt, and nutrient inputs to the East China Sea. Impinging eddies and typhoons are two of the principal causes of variability in the Kuroshio. This study's models are more consistent with the observed Kuroshio than with high-frequency radar measurements.

INTRODUCTION

The Kuroshio has substantial momentum and transports distinct water masses, heat, salt, and larval fish from east of the Philippines to southeast of Japan, greatly influencing regional oceanography, fisheries, and climate along its route. Areas that will benefit from a fuller understanding of the Kuroshio range from fisheries management to climate and weather prediction. East of Taiwan, the Kuroshio is roughly midway through its 3,000 km journey from ~12°N to ~35°N in the western North Pacific. Knowledge of the mean state and variability of this section of the Kuroshio is crucial to delineating its downstream variability in the East China Sea and in waters south of Japan (Andres et al., 2015, in this issue).

Kuroshio formation takes place from Luzon Strait to the region northeast of Taiwan, and it becomes a relatively stable current in the East China Sea (Nitani, 1972). Using two years of observations along the World Ocean Circulation Experiment (WOCE) PCM-1 line that runs from northeast of Taiwan to Ishigaki Island, Japan, Johns et al. (2001), Zhang et al. (2001), and Yang et al. (1999) concluded that the mean volume transport across PCM-1 was 21 Sv (1 Sv = 10^6 m^3 s^{-1}) with a variability of 10 Sv and strong 100-day fluctuations, presumably caused by impinging mesoscale eddies from the east. Using historical hydrography and recent velocity measurements obtained from Taiwan's Ocean Data Bank (http://www.odb.ntu.edu.tw), Liang et al. (2003) and Rudnick et al. (2011) describe the climatological structure of the Kuroshio off the east coast of Taiwan. There have been no comprehensive, systematic observations of the Kuroshio east of Taiwan since the WOCE PCM-1 observation period from 1996 to 1997; thus, progress in understanding the current in this area has been at a standstill since then.

It was not until the Observations of the Kuroshio Transports and their Variability (OKTV) program, sponsored by the Ministry of Science and Technology, Republic of China (Taiwan), from 2012 to 2015 (Jan et al., 2015), that multiple platforms observed the Kuroshio in detail along three zonal transects east of Taiwan (Figure 1). The OKTV program, in collaboration with the US Office of Naval Research-sponsored Origins of Kuroshio and Mindanao Current (OKMC) program, aimed to measure the volume, heat, salt, and nutrient transports at the northern transect (Figure 1) and to quantify the flow pattern and hydrographic variability of the Kuroshio east of Taiwan. Using OKTV-collected ship data, Jan et al. (2015) found that the Kuroshio

core transport ranged from 10.46 Sv to 22.92 Sv, the Kuroshio maximum velocity was between 0.7 m s^{-1} and 1.4 m s^{-1}, and the offshore distance of this maximum velocity position varied greatly from 12 km to 103 km. The associated heat transport referenced to 0°C was $0.838–1.793 \times 10^{15}$ W, and the salt transport was $345.0–775.9 \times 10^6$ kg s^{-1}. Analysis of the Kuroshio water mass indicated dominance of South China Sea Tropical Water (SCSTW) on the onshore side (in the upper 250 m), Kuroshio Tropical Water (KTW) in the main stream, and West Philippine Sea Tropical Water (WPSTW) on the current's offshore flank. The intermediate waters have more complicated origins than do the tropical waters.

This study extends the work of Jan et al. (2015) by analyzing the extensive data set obtained from all of the observational platforms during the OKTV program, and examining the time mean and standard deviation of the velocity and hydrographic structures along the three transects and the variations of water masses associated with the Kuroshio. We discuss the dynamic causes of Kuroshio variability, particularly mesoscale eddies and typhoons. To further evaluate the accuracy of high frequency (HF) radar observations and model simulations of the Kuroshio, HF radar observed surface currents and Kuroshio models are compared with directly measured velocities.

OBSERVATIONAL PLATFORMS

The OKTV program conducted repeated ship surveys and deployed moored instruments, drifters, and HF radars concurrently to observe the Kuroshio and its variability east of Taiwan. The ship-based survey included hydrographic measurements using conductivity-temperature-depth (CTD) sensors and velocity measurements using shipboard and lowered acoustic Doppler current profilers (Sb-ADCPs and LADCPs). The moored instruments included ADCPs and pressure-sensor-equipped inverted echo sounders (PIESs). The analyses of

the multiple in situ data sets were supplemented with satellite sea surface height anomaly (SSHA) data obtained from Archiving, Validation and Interpretation of Satellite Oceanographic data (AVISO; http://www.aviso.oceanobs.com) and Surface Velocity Program (SVP) drifter data extracted from the Global Drifter Program (Maximenko et al., 2013) to examine the influence of eddies on the Kuroshio.

Repeated ship surveys were conducted along the KTV1 (~23.75°N), KTV2 (22.75°N), and KTV3 (22°N) transects

(Figure 1); hydrographic stations 8, 13, and 15 (dots in Figure 1) were located along KTV1, KTV2, and KTV3, respectively. In total, 18 cruises were conducted aboard R/Vs *Ocean Researcher I, III,* and *V* (hereafter *OR1, OR3,* and *OR5*) between September 2011 and June 2015. Figure 1 also plots the time periods of the survey cruises. Each of the three vessels was equipped with a 75 kHz Sb-ADCP measuring the velocity profile in roughly the upper 600 m along the cruise track. The Sb-ADCP measured velocity, which was averaged every two minutes in 8 m

vertical bins. The concurrent model-produced barotropic tidal currents (Jan et al., 2002) were subtracted from the raw Sb-ADCP data, and the de-tided data were subsequently averaged into 30 min time intervals. The LADCP is composed of two 300 kHz ADCPs with a downward-looking master and an upward-looking slaver. Velocity transects were interpolated using both averaged Sb-ADCP and LADCP data for the upper 16 m to 600 m and by using only LADCP data below 600 m at 8 m intervals for the entire water column. The velocity above 16 m was assumed to be the same as that at 16 m depth. The procedures of the CTD/LADCP measurements and associated data processing are detailed in Jan et al. (2015). Here, we present statistics drawn from velocity and hydrography profiles in the upper 500 m of the three transects.

Three sets of upward-looking 75 kHz ADCP moorings were deployed along the KTV1 transect at stations A1, A2, and A3 (solid orange squares in Figure 1), spanning about 70 km and approximately 50%–75% of the width of the Kuroshio main stream (defined by Jan et al., 2015). The velocity profile was measured between 50 m and 500 m depth at five-minute intervals in 8 m vertical bins from November 2012 to October 2014 (Figure 1). To calculate the volume transport through the A1–A3 section, velocities between the sea surface and 50 m depth were assumed to be equal to the velocity measured at 50 m. This study only presents time series of daily volume transport. A detailed analysis of the ADCP data is being prepared by author Chang and colleagues.

Six PIESs were deployed along the KTV1 line and along 123°E (green triangles in Figure 1) from November 2012 to October 2014 to investigate the variability of pycnocline depth across the Kuroshio and the coherence of meridional and zonal variations between the two lines. PIESs measures bottom pressure and vertical round-trip acoustic travel time (τ) between the instrument (moored on the seabed in a rigid anchor
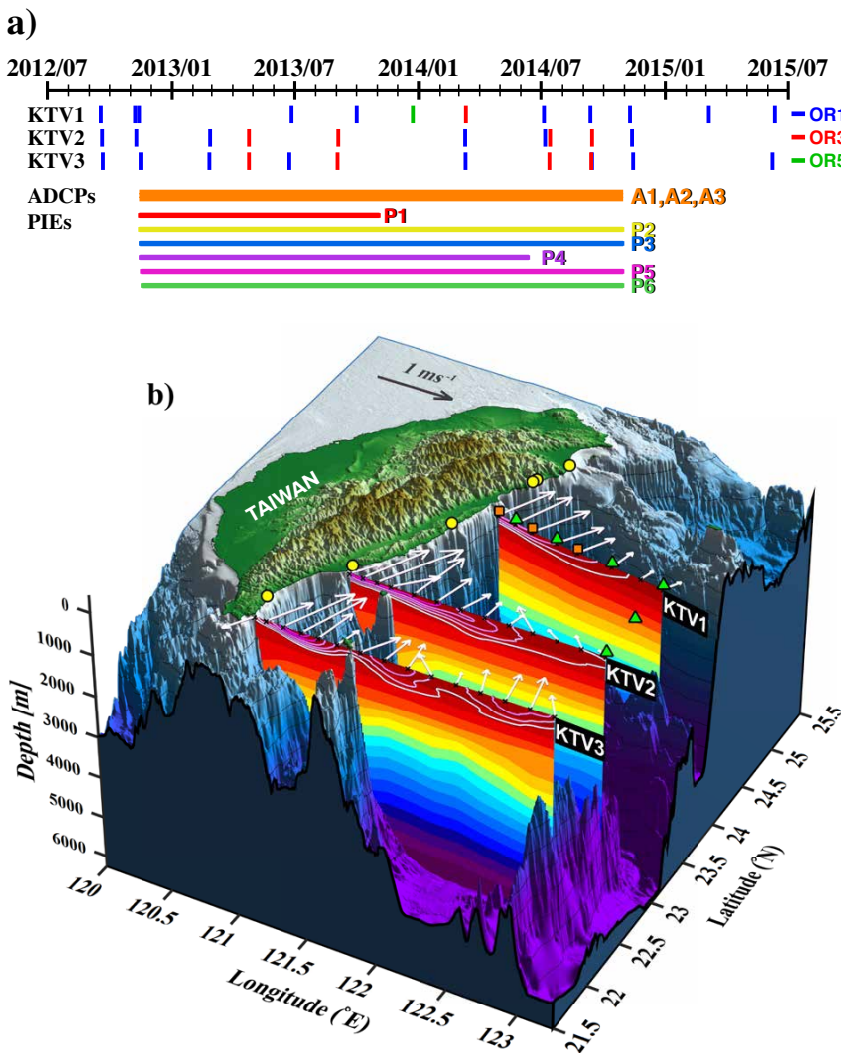

FIGURE 1. (a) Timeline showing the observational periods of the Observations of the Kuroshio Transports and their Variability (OKTV) program ship surveys, moored acoustic Doppler current profilers (ADCPs), and pressure-sensor-equipped inverted echo sounders (PIESs). (b) Three-dimensional perspective view of the mean structure of the Kuroshio (the colors represent temperature and the contours poleward velocity) along the KTV1, KTV2, and KTV3 transects overlaid with the 16 m depth velocity (white vectors) obtained from Sb-ADCP observations east of Taiwan. Black dots indicate the hydrographic sampling locations, solid orange squares the moored ADCPs, solid green triangles the PIES locations, and solid yellow circles the HF radar sites.

stand) and the overlying sea surface. The technology and applications of PIES are delineated in Rossby (1969), Watts and Rossby (1977), Watts et al. (2001), and Andres et al. (2008). In this study, 800 dbar was used as a reference level, and the PIES-measured τ at each site was converted to τ_{800}. Then, τ', the deviation of τ_{800} from its time mean, was converted to the pycnocline depth (d_{pyc}) and used to measure the Kuroshio's response to impinging eddies and typhoons at the PIES array. Details of the PIES observations and associated data processing are described in Tsai et al. (2015).

Data acquired from six HF radar sites along the east coast of Taiwan (locations indicated by yellow circles in Figure 1) during 2013 were used to map the sea surface currents. The two northernmost radar sites are operated by the National Taiwan University/Naval Academy joint program, and the remaining four sites are operated by the Taiwan Ocean Research Institute. Each site was equipped with the coastal ocean dynamic application radar (CODAR) long-ranger model, with a practical spatial observation radius up to 220 km and horizontal resolution around 8 km in the radial direction and 2° in azimuth. CODAR signal processing is explained in Lipa et al. (2006). After subtracting the noise (from, e.g., ionosphere effects and signals reflecting from artificial structures), we combined the radial velocities from the six radar sites to obtain the sea surface currents (u, v) east of Taiwan. To verify CODAR performance, these results were compared with the Sb-ADCP and SVP drifter observations, and the averaged coefficient of determination (r^2) was 0.74 (Fang et al., 2011; Lee, 2015).

TIMCOM MODEL

The model simulation was based on the Taiwan Multi-scale Community Ocean Model (TIMCOM; Tseng et al., 2012; Young et al., 2012; Shen et al., 2014). The model domain covered the entire North Pacific Ocean from 30°S to 60°N and 100°E to 80°W. A dual-grid approach was

implemented so that 1/8° resolution was used in the domain west of 150°E, and 1/4° resolution was used in the domain east of 150°E. Further details on the model can be found in Tseng et al. (2012). A major difference in the setup used in this study was that the updated 30 arc sec General Bathymetric Chart of the Oceans (GEBCO) data (available at http://www.gebco.net) replaced the ETOPO2 bathymetry. The vertical resolution was linear-exponentially stretched by 26 levels in both the coarser and finer grids.

The 2013–2014 hindcast simulation was driven by the six-hourly 0.125° ERA-interim atmospheric reanalysis product (Dee et al., 2011). River runoff was based on an updated version of the Global River Flow and Continental Discharge Dataset (Dai and Trenberth, 2002; Dai et al., 2009). The simulated 2013 Kuroshio was analyzed and compared with observations from OKTV.

MEAN STATE AND VARIABILITY OF THE KUROSHIO

Figure 2 illustrates the time mean and standard deviation of velocity (u, v), and temperature and salinity analyzed from ship survey data in the upper 500 m along the KTV1, KTV2, and KTV3 transects. The mean Kuroshio velocity transect (v) showed two velocity maxima on the KTV3 and KTV2 lines, with the Kuroshio's primary velocity core on the onshore side (Figure 2b). The mean maximum velocity was ~1.2 m s^{-1}. Along KTV1, the mean velocity structure became a single velocity maximum of ~1 m s^{-1} (Figure 2b). K.-C. Yang et al. (2015, in this issue) suggest two mechanisms that may cause the two velocity maxima (dual-core velocity structure). One is the intrusion of the Kuroshio into the South China Sea (SCS) through Luzon Strait, which normally occurs during the northeast monsoon in winter. The other is the dissipation of westward-propagating anticyclonic eddies, which result in an offshore core along the Kuroshio's east flank. The standard deviation of the directly measured velocity (σ_v) was ~0.4 m s^{-1}, which is

about 33% of the mean maximum velocity in the main stream of the Kuroshio. During the two-year observational period, seven mesoscale eddies were detected from the SSHA and PIES travel-time-derived pycnocline depth anomaly (Tsai et al., 2015). The larger standard deviation in the directly measured (u, v) near the eastern end of the KTV2 and KTV3 transects (122.5°E–122.8°E) is presumably affected by westward-propagating eddies impinging on the offshore (eastern) side of the Kuroshio during the ship surveys. Figure 2a suggests that the mean zonal velocity (u) was about one-quarter of the mean poleward velocity along the three transects, with relatively large variability (σ_u ~0.4 m s^{-1}). The greatest variability in u ($\sigma_u > 0.6$ m s^{-1}) occurred along KTV2 immediately north of Green Island, which is located about 33 km off of Southeast Taiwan.

Isotherms are tilted upward toward the onshore flank of the Kuroshio (Figure 2c) as is typical for a hydrographic transect of a geostrophic current. The geostrophic current velocity estimated using OKTV CTD data and the thermal wind relation could be 6%–30% different from the directly measured velocity along the KTV1 transect (Jan et al., 2015). These differences mean that the directly measured Kuroshio velocity has a sizable ageostrophic component. The standard deviation of temperature, σ_T, was 2°C in the upper 100 m of the KTV1 transect. The highest σ_T, observed between 400 m and 500 m depth from 122.6°E to 122.9°E along the KTV3 line, was likely due to the influence of the same eddies that affected the velocity measurements (σ_u along KTV3 in Figure 2a). The mean salinity was fairly low (<34) in the upper 50 m on the onshore side of the Kuroshio (Figure 2d). The salinity maximum, indicating tropical waters, was located between 100 m and 200 m depth. The large variability in salinity with $\sigma_S > 0.4$ was mostly in the upper 50–100 m along the three transects (Figure 2d).

Observations collected by the OKTV program provide a new and invaluable

data set that can be used to validate both the performance of the model simulation and the accuracy of HF radar observations of the Kuroshio. The time mean and standard deviation of CODAR-observed sea surface currents and TIMCOM simulated currents at the shallowest level (~3 m depth) during 2013 were compared with the values estimated from all of the Sb-ADCP observed currents at 16 m depth along KTV1, KTV2, and KTV3 (Figure 3). The magnitude of the mean velocity estimated from the CODAR observations is about two-thirds as strong

as that estimated from the Sb-ADCP observations in the Kuroshio main stream (Figure 3a). The mean flow direction of the CODAR observations is comparable to that of the ship observations along KTV2 and KTV3, but is rotated ~10°–20° clockwise from that of the ship observations at the KTV1 transect (Figure 3a). Note that the time mean of CODAR-observed surface currents (left panel of Figure 3a) seemingly does not satisfy the conservation of volume in the surface layer. In addition to errors caused by the ionosphere effect and reflected signals from

artificial structures, the difference in the calibration of radar systems may result in inconsistencies among their observed sea surface velocities, something that merits further examination. In the Kuroshio main stream, both the mean magnitudes and the directions of the TIMCOM simulations were similar to those of the ship observations (Figure 3b). The standard deviation of directly measured surface velocity (σ_u and σ_v) was generally larger than that calculated from the CODAR observations and TIMCOM simulations (right panels in Figure 3), particularly in
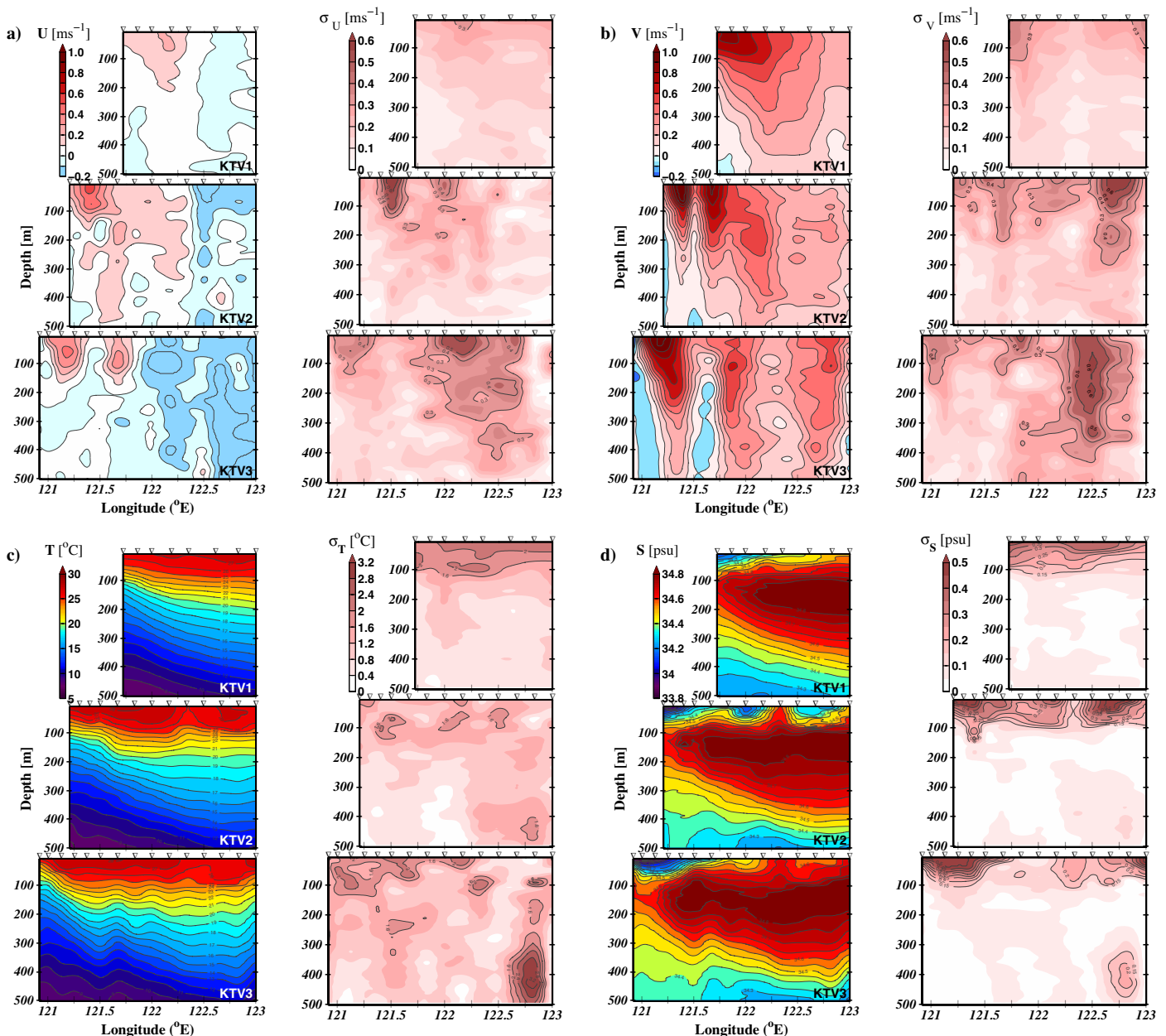

FIGURE 2. Time mean and standard deviation of velocity (a) zonal component *u*, (b) meridional component *v*, and (c) temperature and (d) salinity calculated from the ship-based observations collected by the OKTV program along the KTV1, KTV2, and KTV3 transects.

the eastern half of the KTV2 and KTV3 lines. The lack of westward-propagating mesoscale eddies or appropriate eddy-Kuroshio interactions in the model may cause this model-data discrepancy. There are many other possible causes for the differences between measured and modeled velocities, including differences in observational methods, model grid resolutions, and model parameterizations. The differences between the Sb-ADCP measured velocity and the CODAR measured surface currents, particularly near the easternmost area of our survey, may be caused by attenuation of the reflected signals received by the HF radar at a remote distance. A detailed discussion on the causes of mismatches among different observational platforms or between the model-produced and the observed currents is beyond the scope of this paper.

WATER MASSES ASSOCIATED WITH THE KUROSHIO

The hydrographic measurements from the 18 OKTV cruises provide a view of the complex distribution and interactions of water masses east of Taiwan. Here, we divide the region into southwestern, southeastern, northwestern, and northeastern domains (Figure 4) to highlight the influence of the South China Sea water masses on the area west of the Kuroshio and the role of the shallow topography southeast of Taiwan. The potential temperature-salinity (θ-S) profiles of casts within all four domains were plotted separately over generic θ-S curves for Kuroshio Water, South China Sea Water, and North Pacific Water, as defined in Mensah et al. (2014). These waters can be classified as tropical and intermediate waters, with the 25.8 kg m^{-3} isopycnal marking their interfaces (Figure 4). The tropical waters are distinguished by salinity maxima (S_{max}) at ~150 m depth (Rudnick et al., 2011), with values of 35.06, 34.85, and 34.60 for the KTW, NPTW, and SCSTW, respectively. The salinity minimum (S_{min}) typical of the intermediate waters is found around 500 m to 600 m depth. Salinity minima for Kuroshio Intermediate

Water (KIW), North Pacific Intermediate Water (NPIW), and South China Sea Intermediate Water (SCSIW) are 34.31, 34.21, and 34.41, respectively.

Regarding the tropical waters, the two western boxes (Figure 4a,b) display the highest variability in water properties due to the presence of both SCSTW and NPTW/KTW. The existence of low S_{max} waters in these regions is explained by the advection of SCSTW along the western flank of the Kuroshio (e.g., Mensah et al., 2014; Jan et al., 2015). Jan et al. (2015) demonstrate that the northward flow of SCSTW is intermittent east of Taiwan, and Mensah (2015) suggests that

westward Kuroshio intrusion in Luzon Strait is a likely factor for the reduction of the northward flow of SCSTW. The saltier S_{max} waters in the western boxes are likely variations of KTW, whose S_{max} decreased after encountering vigorous mixing in Luzon Strait and becoming more like NPTW (Mensah et al., 2014). The two eastern boxes (Figure 4c,d) display lower variability, with mostly high S_{max} waters present in these areas. Mesoscale eddies may advect saltier variations of NPTW (Jan et al., 2015), and some KTW may be transported northward without passing through Luzon Strait, thus keeping its typical high S_{max} (Mensah, 2015).
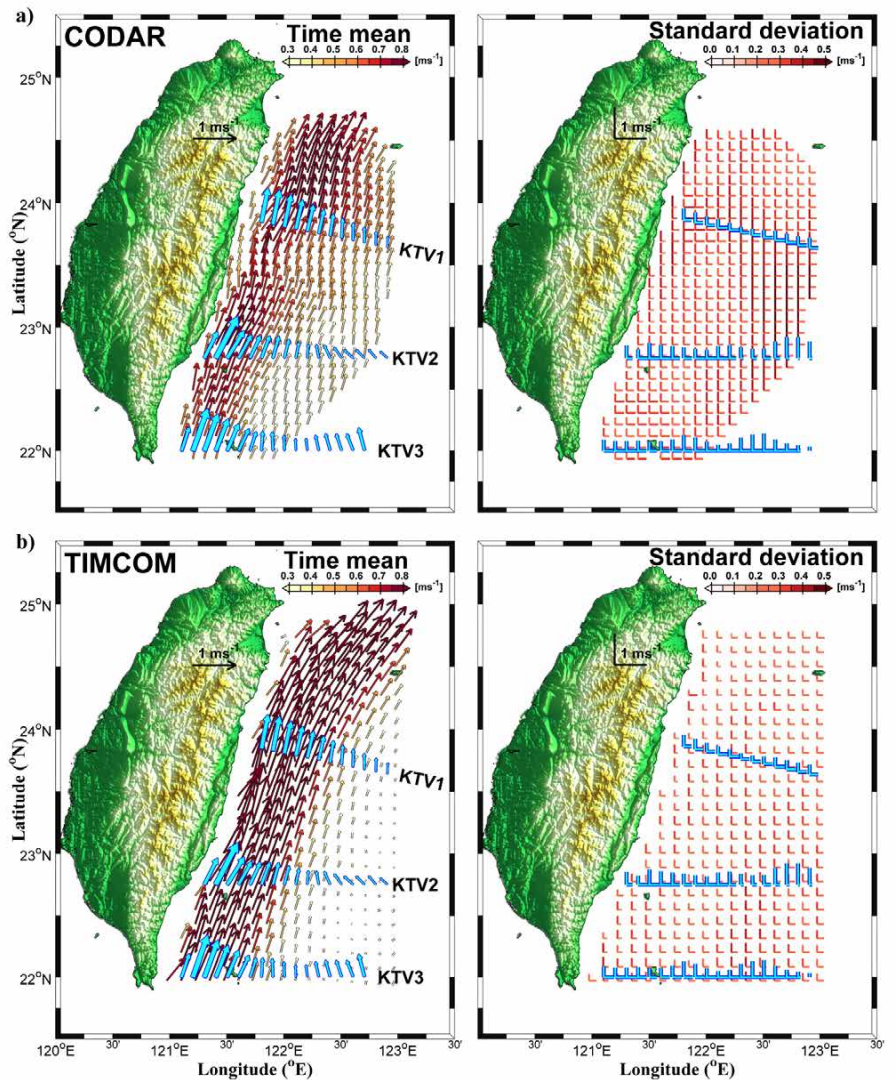

FIGURE 3. Time mean and standard deviation of the surface current velocity from a year (2013) of (a) coastal ocean dynamic application radar (CODAR) observations, and (b) Taiwan Multi-scale Community Ocean Model (TIMCOM) simulations, overlain with time mean (left panels) and standard deviation (right panels) of all available ship-based ADCP observed currents at 16 m depth across the KTV1, KTV2, and KTV3 transects (blue arrows).

The shallow topography east of Taiwan strongly influences the characteristics of the intermediate waters in the two western boxes (Figure 4a,b). The shallow ridge north-northwest of Green Island prevents SCSIW from flowing north, and only when the Kuroshio current is strong and deep can a salty mix of SCSIW and KIW reach the area east of Taiwan (Mensah et al., 2015). This explains why high S_{min} waters are mostly found in the southwestern box, and no typical SCSIW profiles occur in the northwestern box, where there is a higher proportion of low S_{min} NPIW. This NPIW flows northwestward from the Philippine Sea basin and is usually found below the eastern flank of the Kuroshio (Figure 4c,d), and below

its westward flank when the Kuroshio east of Luzon island is too weak and shallow to transport intermediate water from upstream regions (Mensah et al., 2015).

These results have important implications for the nature of the water masses found further north. Chen and Wang (1998) indicate that traces of the nutrient-rich SCSTW and SCSIW can be found up to southern Japan, but the high variability of the water masses transported east of Taiwan suggests that these waters may be absent from the Japanese shores on many occasions. Characteristics of the waters east of Taiwan must then be key to the explaining the heat and nutrient content variability of the Kuroshio waters observed south of Japan.

ORIGINS OF VARIABILITY IN THE KUROSHIO

Figure 5a shows SSHA overlain with CODAR-measured surface currents on May 16, 2013, when a cyclonic eddy (CE1) with negative SSHA was centered southeast of Taiwan at 22.5°N, 123°E. CODAR-measured surface currents roughly indicate the influence of CE1 on the surface current pattern in the Kuroshio region; the northward surface current of the Kuroshio was weakened at ~24°N and reversed from north to south off the east coast of Taiwan between 22°N and 23°N. During the period of CE1 influence in May 2013, an SVP drifter (red-line trajectory) followed the peripheral currents of this eddy, traveling cyclonically
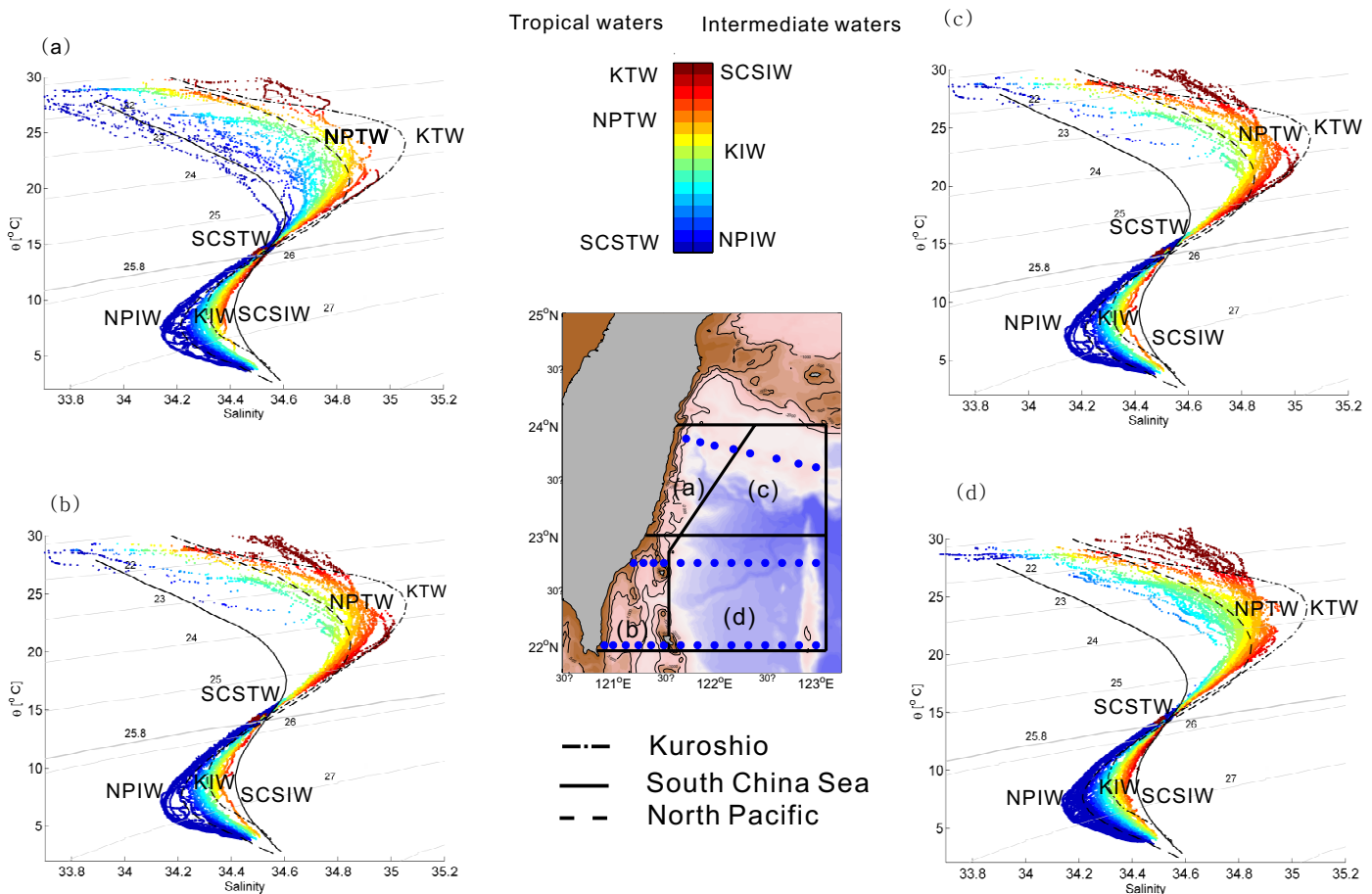

FIGURE 4. (center) Bathymetry east of Taiwan showing locations of the 36 OKTV stations (blue dots) and the authors' geographical divisions (black lines) along and across the Kuroshio. The corresponding θ-S curves obtained from the OKTV cruises in the four regions are plotted in panels a, b, c, and d. The dash-dotted, solid, and dashed black lines represent the reference θ-S curves for the Kuroshio, South China Sea, and North Pacific Waters, respectively, as defined in Mensah et al. (2014). The color scale represents the salinity of the water relative to the highest salinity among the reference tropical and intermediate water masses. The typical salinity maximum (minimum) values of Kuroshio Tropical Water (KTW), North Pacific Tropical Water (NPTW), South China Sea Tropical Water (SCSTW), Kuroshio Intermediate Water (KIW), North Pacific Intermediate Water (NPIW), and South China Sea Intermediate Water (SCSIW) are indicated in the colored bar. The bold solid gray isopycnal marks the limit of influence of tropical and intermediate waters.

from the southern tip of Taiwan and then further east.

Figure 5b shows the SSHA and CODAR measured surface currents on November 23, 2013, when another cyclonic eddy (CE2) was located southeast of Taiwan. Indeed, this negative SSHA system stalled in this region for three months (October–December 2013), and the velocity structure across the Kuroshio along the KTV1 transect was directly observed (Jan et al., 2015). The associated flow pattern was a large cyclonic Kuroshio meander east of Taiwan; Jan et al. (2015) discuss the underlying dynamics. A corresponding SVP drifter trajectory (red-line trajectory in Figure 5b) crossed the Kuroshio main stream with the cyclonic currents of CE2, passing from the offshore side of the Kuroshio to the east coast of Taiwan.

The influences of CE1 and CE2 were also recorded by the moored ADCP and PIES. The time series of pycnocline depth at the six PIESs in Figure 6b and the volume transport calculated using the three ADCPs at A1, A2, and A3 in Figure 6c show the influence of these two cyclonic eddies. PIES observations suggest that a heaved thermocline associated with each eddy's SSHA low (particularly on the offshore side of the current) as each arrived on the Kuroshio's offshore edge. In addition, the transports across A1–A3 decreased from 12 Sv to 5 Sv due to each cyclonic eddy's arrival (see a zoom-in for the variations of pycnocline depth and transport during CE1 in the inset above Figure 6b). The influence of impinging eddies on the SSHA and pycnocline depth across the Kuroshio is detailed in Tsai et al. (2015) using the PIES observations, and is thus not discussed here for brevity.

In addition to eddy influences on Kuroshio variability, typhoons may cause variations, possibly through wind-induced sea surface stress and wind-stress-curl-induced Ekman pumping at a time scale of two to three days. While the impacts of typhoons on the Kuroshio at the shelf break northeast of Taiwan have been widely studied (Chang et al., 2008;

Y.-L. Tsai et al., 2008, 2013; Morimoto et al., 2009), their impacts east of Taiwan are less well studied. The two years of observations from the PIES array east of Taiwan provide an opportunity to look into typhoon influence on the Kuroshio. Figure 6a shows eight typhoon tracks that may have affected the Kuroshio between the northern Luzon Strait and east of Taiwan during 2013 and 2014. Figure 6b shows time series of pycnocline depth (d_{pyc}) from the six PIESs with the period when each typhoon was close to the PIES array, marked with gray vertical lines and the corresponding index number of each typhoon at the top. A close-up of the response of pycnocline depth to, for example, Typhoon Sulik, in the inset above Figure 6b suggests that d_{pyc} and transport decrease during the latter half of a typhoon's influence. The typhoon-induced decrease in d_{pyc} can be further classified into to "small" effects—possibly due to typhoons that passed far from the array (Typhoons 1, 3, 5, and 6; see Figure 6a), and "large" effects due to typhoons that passed closer to the array (Typhoons 2, 4, 7, and 8). Here, the distance between a typhoon and PIESs was coarsely estimated from the shortest distance between the typhoon track and the PIES array. Interestingly, the typhoon-induced decreases of d_{pyc} do not appear to be related directly to the strength of the eight typhoons. The volume transport

calculated from the three ADCPs moored at A1, A2, and A3 decreased by about 2 Sv to 3 Sv during most of the eight typhoons with the exception of Typhoons 4 and 8, during which the transport appears to have increased. The difference in the change of the transport due to typhoon influence may result from the location of the typhoon tracks, which were northward for Typhoons 4 and 8 and are generally northwestward for the other six typhoons.

The observed decrease in d_{pyc} was likely associated with either temperature or salinity (or both) decreases that typically occur above the pycnocline during a typhoon passage. The direct influences of typhoons on the upper ocean include sea surface cooling due to the air-sea heat exchange, salinity decrease due to rainfall, vertical mixing in the water mass due to wind-stress-induced stirring, and uplift of cool subsurface water due to wind-stress-curl-induced Ekman pumping in the upper 100 m. The combination of these processes may be responsible for the decrease in temperature and salinity in the upper layer of the Kuroshio, which increases (decreases) the acoustic travel time (pycnocline depth) obtained from PIES observation due to the dependence of sound speed on temperature and salinity. The changes in the temperature/salinity of the water column across the Kuroshio conceivably lead to variations in its (geostrophic) velocity structure, and,
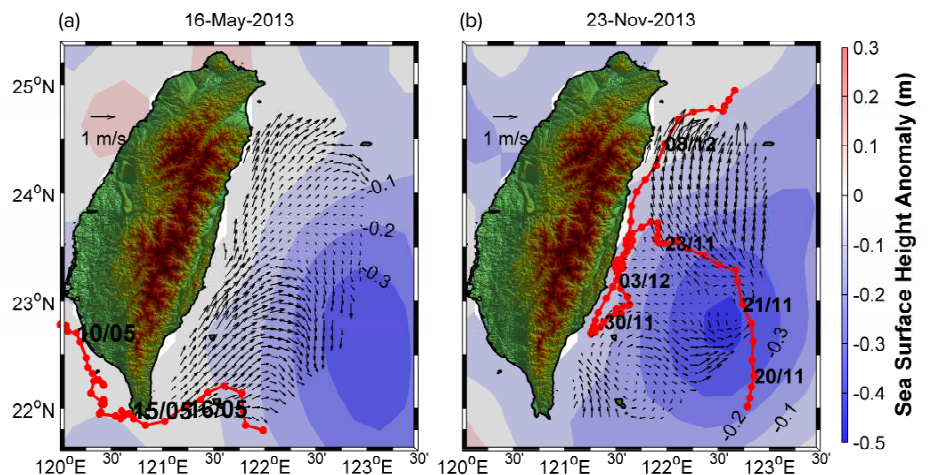

FIGURE 5. Sea surface height anomaly and sea surface currents on (a) May 16 and (b) November 23, 2013. Red lines show the trajectories of the SVP drifters.

in turn, in the volume transport. The dynamics responsible for the typhoon-induced decrease in pycnocline depth and associated short-term variability in the Kuroshio merit more detailed investigation in the future.

CONCLUSION

This study investigated the mean structure and variability of the Kuroshio east of Taiwan primarily based on a new data set obtained from comprehensive field observations using multiple platforms during the OKTV program between September

FIGURE 6. (a) Typhoon tracks that passed near the KTV1 transect during November 2012 and November 2014. (b) Time series of pycnocline depth (d_{pyc}) derived from PIES travel time anomalies (τ') referenced to 800 dbar depth. (c) Daily volume transport across moored ADCP stations A1–A3, representing 50% to 75% of the total Kuroshio core transport defined by Jan et al. (2015). The numbers above the upper frame of panel (b) mark the periods of influence of the eight typhoons listed in the upper-left inset in panel (a). CE1 and CE2 indicate the two cyclonic mesoscale eddies that affected the Kuroshio in May 2013 and November 2013, respectively. The two insets above (b) show a close-up of CE1 and Typhoon Soulik influences on pycnocline depth at each of the PIES stations in (b) and volume transport in (c).

2012 and June 2015. The mean Kuroshio velocity transects showed two velocity maxima along the KTV3 and KTV2 transects, with the primary velocity core on the onshore side of the Kuroshio. The mean maximum velocity was ~1.2 m s^{-1}. The mean velocity structure became a single velocity maximum of ~1 m s^{-1} along the KTV1 transect. The standard deviation of the directly measured poleward velocity (v) was ~0.4 m s^{-1} in the Kuroshio main stream. The mean zonal velocity (u) was about one-quarter of the mean poleward velocity along the three transects, with relatively large variability (standard deviation σ_u ~ 0.4 m s^{-1}). The largest variability in u (σ_u > 0.6 m s^{-1}) occurred along the KTV2 transect immediately north of Green Island.

The water masses associated with the Kuroshio consist of tropical and intermediate waters that originate from the upstream Kuroshio, the South China Sea, and the North Pacific. In the tropical water layer, SCSTW was found mostly on the western side of the Kuroshio, whereas a strongly mixed KTW and NPTW layer was typically found further east. The pronounced variability in tropical waters found on the eastern side of the Kuroshio is likely due to the current's varying paths and to impinging mesoscale eddies. Topography plays a significant role in the circulation and distribution of the deeper waters in the intermediate water layer. Waters of South China Sea and Kuroshio origin are mostly found southeast of Taiwan, up to Green Island. The shallow ridge between the Taiwan coast and Green Island prevents some of the intermediate water from flowing further north, and KIW is found upstream of I-Lan Ridge only when the Kuroshio is strong enough to carry it there. As a result, NPIW was the dominant water mass observed east of Taiwan beyond 23°N.

CODAR, PIES, and ADCP observations supplemented with satellite SSHA and SVP drifter trajectories facilitated the analysis of Kuroshio variability induced by impinging eddies and typhoons. Two cyclonic eddies that impinged on the Kuroshio caused cyclonically moving surface currents in the Kuroshio observed by CODAR and SVP drifters, an increase of acoustic travel time anomalies observed by PIESs due to eddy-induced isopycnal uplift in the upper water column, and a decrease in the volume transport through ADCP mooring sites A1–A3. Typhoons may cause the increases in the acoustic travel time anomaly recorded at the six PIES stations. Transport across the A1–A3 transect decreased during six of eight typhoons that traveled approximately southeast to the northwest in the region. In contrast, transport increased during two northward-moving typhoons.

The unprecedented in situ data set obtained from the OKTV program, augmented by observations from the OKMC Program, is not only crucial for detailed evaluation of Kuroshio variability east of Taiwan but also is useful for validating numerical simulations and surface currents measured by HF radar. 🌀
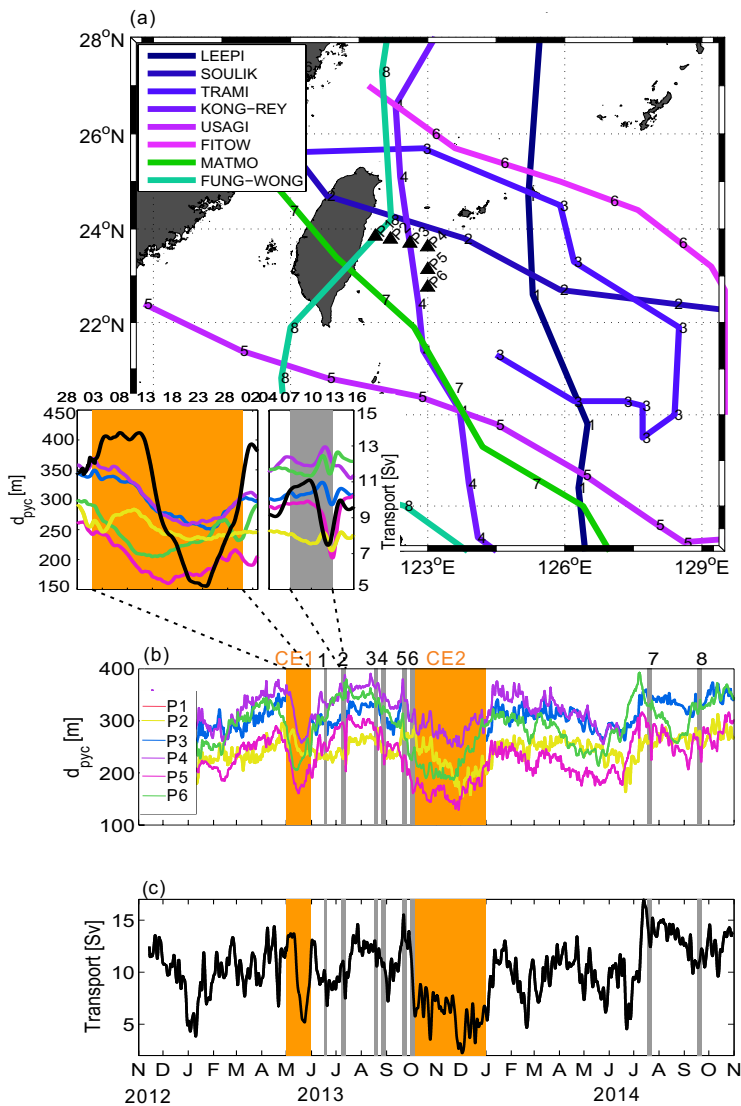
REFERENCES

Andres, M., S. Jan, T.B. Sanford, V. Mensah, L.R. Centurioni, and J.W. Book. 2015. Mean structure and variability of the Kuroshio from northeastern Taiwan to southwestern Japan. *Oceanography* 28(4):84–95, http://dx.doi.org/10.5670/oceanog.2015.84.

Andres, M., M. Wimbush, J.-H. Park, K.-I. Chang, B.-H. Lim, D.R. Watts, H. Ichikawa, and W.J. Teague. 2008. Observations of Kuroshio flow variations in the East China Sea. *Journal of Geophysical Research* 113, C05013, http://dx.doi.org/10.1029/2007JC004200.

Chang, Y., H.-T. Liao, M.-A. Lee, J.-W. Chan, W.-J. Shieh, K.-T. Lee, G.-H. Wang, and Y.-C. Lan. 2008. Multisatellite observation on upwelling after the passage of Typhoon Hai-Tang in the southern East China Sea. *Geophysical Research Letters* 35, L03612, http://dx.doi.org/10.1029/2007GL032858.

Chen, C.T.A., and S.L. Wang. 1998. Influence of intermediate water in the western Okinawa Trough by the outflow from the South China Sea. *Journal of Geophysical Research* 103:12,683–12,688, http://dx.doi.org/10.1029/98JC00366.

Dai, A., T. Qian, K.E. Trenberth, and J.D. Milliman. 2009. Changes in continental freshwater discharge from 1948–2004. *Journal of Climate* 22:2,773–2,792, http://dx.doi.org/10.1175/2008JCLI2592.1.

Dai, A., and K.E. Trenberth. 2002. Estimates of freshwater discharge from continents: Latitudinal and seasonal variations. *Journal of Hydrometeorology* 3:660–687, http://dx.doi.org/10.1175/1525-7541(2002)003<0660:EOFDFC>2.0.CO;2.

Dee, D.P., S.M. Uppala, A.J. Simmons, P. Berrisford, P. Poli, S. Kobayashi, U. Andrae, M.A. Balmaseda, G. Balsamo, P. Bauer, and others. 2011. The ERA-Interim reanalysis: Configuration and performance of the data assimilation system. *Quarterly Journal of the Royal Meteorological Society* 137:553–597, http://dx.doi.org/10.1002/qj.828.

Fang, Y.C., J. Wang, Y.J. Yang, J.C. Mau, K.H. Thia, and M.J. Huang. 2011. Preliminary results of CODAR surface current observations northeast of Taiwan. Pp. 59–77 in *Proceedings of the 2011 International Workshop on Operating System for Marine Environment Monitoring and Forecasting*. Kaohsiung, Taiwan.

Jan, S., C.-S. Chern, and J. Wang. 2002. Transition of tidal waves from the East to South China Seas over the Taiwan Strait: Influence of the abrupt step in the topography. *Journal of Oceanography* 28:837–850, http://dx.doi.org/10.1023/A:1022827330693.

Jan, S., Y.J. Yang, J. Wang, V. Mensah, T.-H. Kuo, M.-D. Chiou, C.-S. Chern, M.-H. Chang, and H. Chien. 2015. Large variability of the Kuroshio at 23.75°N east of Taiwan. *Journal of Geophysical Research* 120:1,825–1,840, http://dx.doi.org/10.1002/2014JC010614.

Johns, W.E., T.N. Lee, D. Zhang, R. Zantopp, C.-T. Liu, and Y. Yang. 2001. The Kuroshio east of Taiwan: Moored transport observations from the WOCE PCM-1 array. *Journal of Physical Oceanography* 31:1,031–1,053, http://dx.doi.org/10.1175/1520-0485(2001)031<1031:TKEOTM>2.0.CO;2.

Lee, C.-Y. 2015. Observation of surface currents using HF radar off the east coast of Taiwan: Data quality control and preliminary results. Master's Dissertation, National Taiwan University, Taipei, Taiwan.

Liang, W.-D., T.Y. Tang, Y.J. Yang, M.T. Ko, and W.-S. Chuang. 2003. Upper-ocean currents around Taiwan. *Deep Sea Research Part II* 50:1,085–1,105, http://dx.doi.org/10.1016/S0967-0645(03)00011-0.

Lipa, B.J., B. Nyden, D.S. Ullman, and E. Terrill. 2006. SeaSonde radial velocities: Derivation and internal consistency. *IEEE Journal of Oceanic Engineering* 31:850–861, http://dx.doi.org/10.1109/JOE.2006.886104.

Maximenko, N., R. Lumpkin, and L. Centurioni. Ocean surface circulation. Pp. 283–304 in *Ocean Circulation and Climate: A 21st Century Perspective*. G. Siedler, S.M. Griffies, J. Gould, and J.A. Church, eds, Academy Press, Oxford, UK.

Mensah, V. 2015. Evolution of the water masses associated with the Kuroshio from Luzon Strait to east of Taiwan. PhD Dissertation, National Taiwan University, Taipei, Taiwan.

Mensah, V., S. Jan, M.-H. Chang, and Y.-J. Yang. 2015. Intraseasonal to seasonal variability of the intermediate waters along the Kuroshio path east of Taiwan. *Journal of Geophysical Research* 120:5,473–5,489, http://dx.doi.org/10.1002/2015JC010768.

Mensah, V., S. Jan, M.-D. Chiou, T.-H. Kuo, and R.-C. Lien. 2014. Evolution of the Kuroshio Tropical Water from the Luzon Strait to the east of Taiwan. *Deep Sea Research Part I* 86:68–81, http://dx.doi.org/10.1016/j.dsr.2014.01.005.

Morimoto, A., S. Kojima, S. Jan, and D. Takahashi. 2009. Movement of the Kuroshio axis to the northeast shelf of Taiwan during typhoon events. *Estuarine, Coastal and Shelf Science* 82:547–552, http://dx.doi.org/10.1016/j.ecss.2009.02.022.

Nitani, H. 1972. Beginning of the Kuroshio. Pp. 129–163 in *Kuroshio: Its Physical Aspects*. H. Stommel and K. Yoshida, eds, University of Tokyo Press, Tokyo, Japan.

Rudnick, D.L., S. Jan, L. Centurioni, C.M. Lee, R.-C. Lien, J. Wang, D.-K. Lee, R.-S. Tseng, Y.Y. Kim, and C.-S. Chern. 2011. Seasonal and meso-scale variability of the Kuroshio near its origin. *Oceanography* 24:52–63, http://dx.doi.org/10.5670/oceanog.2011.94.

Rossby, T. 1969. On monitoring depth variations of the main thermocline acoustically. *Journal of Geophysical Research* 74:5,542–5,546, http://dx.doi.org/10.1029/JC074i023p05542.

Shen, M.-L., Y.-H. Tseng, S. Jan, C.-C. Young, and M.-D. Chiou. 2014. Long-term variability of the Kuroshio transport east of Taiwan and the climate it conveys. *Progress in Oceanography* 121:60–73, http://dx.doi.org/10.1016/j.pocean.2013.10.009.

Tsai, C.-J., M. Andres, S. Jan, V. Mensah, T. Sanford, R.-C. Lien, and C. Lee. 2015. Eddy-Kuroshio interaction processes revealed by mooring observations off Taiwan and Luzon. *Geophysical Research Letters* 42:8,098–8,105, http://dx.doi.org/10.1002/2015GL065814.

Tsai, Y.-L., C.-S. Chern, S. Jan, and J. Wang. 2013. Numerical study of cold dome variability induced by Typhoon Morakot (2009) off northeastern Taiwan. *Journal of Marine Research* 71:109–132, http://dx.doi.org/10.1357/002224013807343434.

Tsai, Y.-L., C.-S. Chern, and J. Wang. 2008. Typhoon induced upper ocean cooling off northeastern Taiwan. *Geophysical Research Letters* 35, L14605, http://dx.doi.org/10.1029/2008GL034368.

Tseng, Y.H., M.L. Shen, S. Jan, D.E. Dietrich, and C.P. Chiang. 2012. Validation of the Kuroshio current system in the dual-domain Pacific Ocean model framework. *Progress in Oceanography* 105:102–124, http://10.1016/j.pocean.2012.04.003.

Watts, D.R., and H.T. Rossby. 1977. Measuring dynamic heights with inverted echo sounders: Results from MODE. *Journal of Physical Oceanography* 7:345–358, http://dx.doi.org/10.1175/1520-0485(1977)007<0345:MDHWIE>2.0.CO;2.

Watts, D.R., C. Sun, and S. Rintoul. 2001. A two-dimensional gravest empirical mode determined from hydrographic observations in the Subantarctic Front. *Journal of Physical Oceanography* 31:2,186–2,209, http://dx.doi.org/10.1175/1520-0485(2001)031<2186:ATDGEM>2.0.CO;2.

Yang, K.-C., J. Wang, C.M. Lee, B. Ma, R.-C. Lien, S. Jan, Y.J. Yang, and M.-H. Chang. 2015. Two mechanisms cause dual velocity maxima in the Kuroshio east of Taiwan. *Oceanography* 28(4):64–73, http://dx.doi.org/10.5670/oceanog.2015.82.

Yang, Y., C.-T. Liu, J.-H. Hu, and M. Koga. 1999. Taiwan current (Kuroshio) and impinging eddies. *Journal of Oceanography* 55:609–617, http://dx.doi.org/10.1023/A:1007892819134.

Young, C.-C., Y.-H. Tseng, M.-L. Shen, Y.-C. Liang, M.-H. Chien, and C.-H. Chien. 2012. Software development of the Taiwan Multi-scale Community Ocean Model (TIMCOM). *Environmental Modelling and Software* 38:214–219, http://dx.doi.org/10.1016/j.envsoft.2012.05.017.

Zhang, D., W.E. Johns, T.N. Lee, C.-T. Liu, and R. Zantopp. 2001. The Kuroshio east of Taiwan: Modes of variability and relationship to interior meso-scale eddies. *Journal of Physical Oceanography* 31:1,054–1,074, http://dx.doi.org/10.1175/1520-0485(2001)031<1054:TKEOTM>2.0.CO;2.

AUTHORS

Yiing Jang Yang (yjyang67@ntu.edu.tw) is Associate Professor, **Sen Jan** is Professor, **Ming-Huei Chang** is Assistant Professor, **Joe Wang** is Professor, **Vigan Mensah** is Postdoctoral Researcher, **Tien-Hsia Kuo** is Ocean Data Bank Member, **Cheng-Ju Tsai** is Research Assistant, and **Chung-Yaung Lee** is Research Assistant, all at the Institute of Oceanography, National Taiwan University, Taipei, Taiwan. **Magdalena Andres** is Associate Scientist, Woods Hole Oceanographic Institution, Woods Hole, MA, USA. **Luca R. Centurioni** is Associate Researcher, Scripps Institution of Oceanography, University of California, San Diego, La Jolla, CA, USA. **Yu-Heng Tseng** is Project Scientist, National Center for Atmospheric Research, Boulder, CO, USA. **Wen-Der Liang** is Associate Professor, Department of Marine Science, Naval Academy, Kaohsiung, Taiwan. **Jian-Wu Lai** is Research Fellow, Taiwan Ocean Research Institute, National Applied Research Laboratories, Kaohsiung, Taiwan.